

Experimental review of devices to artificially thicken wind tunnel boundary layers

J.E. Sargison¹, G.J. Walker¹, V. Bond², G. Chevalier²

¹School of Engineering

University of Tasmania, Private Bag 65, Hobart, Tasmania, 7001, AUSTRALIA

²Ecole Polytechnique de l'Universite de Nantes, FRANCE

Abstract

Three devices that artificially increase the thickness of the boundary layer in a wind tunnel working section have been tested. These included a serrated fence to disturb the flow, and the use of various secondary jet arrays injected into the boundary layer through the bounding surface. Momentum and turbulence profiles in the boundary layer downstream from the thickening devices were measured. The greatest boundary layer thickness was achieved using an array of varying diameter crossflow jets with the jet diameter reducing with distance downstream. However, the fence thickener and a plate with varying jets increasing in diameter downstream produce a boundary layer with momentum and turbulence profiles more typical of a natural equilibrium boundary layer.

Introduction

Aeronautical wind tunnels are generally designed to minimise the thickness of the boundary layer on the wall in the working section, in order to maximise flow uniformity. However, there are occasions when such wind tunnels are used for non-aeronautical research and a thicker boundary layer is required in order to simulate the physical phenomenon being modelled. A typical application of the present work is to model the boundary layer at the stern of a high-speed catamaran vessel for studies of the flow in flush type waterjet propulsion intakes [1]. Other applications include modelling the atmospheric boundary layer for studies of wind turbine performance.

Atmospheric scale boundary layer simulations in wind engineering use isolated spires of height equal to the thickened boundary layer thickness to introduce the momentum deficit [6]. However this technique may introduce undesirable spanwise variations in the flow. A previous study of techniques to artificially thicken the boundary layer [2] demonstrated the usefulness of arrays of crossflow jets and boundary layer fences. That work has been expanded to include a different, larger boundary layer fence geometry, and the use of an array of varying diameter jets with the large jets downstream. In addition the development of the thickened boundary layer has been studied in more detail by measuring the turbulence and momentum profiles at four planes downstream from the thickener location.

Nomenclature

B Constant
 H Shape factor = δ^*/θ
 K Constant
 Q Total flow rate (m^3/s)
 Re_δ Reynolds number = $\rho U \delta / \nu$
 U Mainstream velocity (m/s)
 c_f skin friction coefficient
 q Flow rate per metre width ($\text{m}^3/\text{s}/\text{m}$)
 u Velocity (m/s)
 $u^+ = u/u^*$

u^* Shear velocity = $(\tau_w / \rho)^{1/2}$

$y^+ = y u^* / \nu$

y Distance from wall (mm)

δ^* Boundary layer displacement thickness

δ Total boundary layer thickness based on 99% velocity

θ Boundary layer momentum thickness

ν Kinematic viscosity (m^2/s)

ρ Density (kg/m^3)

τ_w Wall shear stress

Experimental Technique

Boundary layer thickening devices

The devices used to disturb the boundary layer are shown in Figures 1-3. The devices were installed immediately upstream of the wind tunnel working section, in a location where the natural boundary layer was fully turbulent with a total boundary layer thickness of 16.7mm, $Re_\theta = 1510$. The natural boundary layer thickness at the midplane of the wind tunnel working section was 22.4 mm, $Re_\theta = 5160$.

The fence thickener was inserted into the wind tunnel with the triangular 'spikes' angled at 40° to the wind tunnel wall and their tips pointing downstream. The spikes were at a pitch of 20 mm and 20 mm high in the plane of the spike. The regular and varying hole thickeners were connected to an intake pipe with bell mouth nozzle to measure the flow rate of air ingested into the working section. The plates were located in the sidewall of the wind tunnel, with the downstream edge of the plate 100mm upstream from the start of the wind tunnel working section. The regular hole plate had a hole diameter of 2.3 mm at a pitch of 6.3 mm. The varying hole plate had hole diameters 10, 7.5, 5.5, 4, 3, 2, 1.5 mm (Table 1). The standard installation of the varying holes plate was to have the largest diameter holes upstream. This plate was also tested in a reversed configuration, with the largest holes downstream.



Figure 1a. Fence thickener.

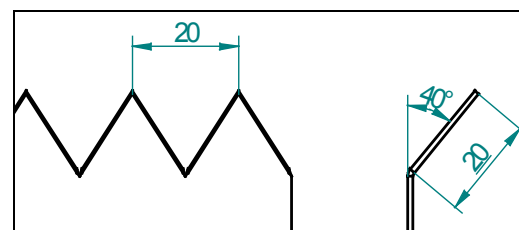


Figure 1b: Fence 'spike' geometry (dimensions in mm).

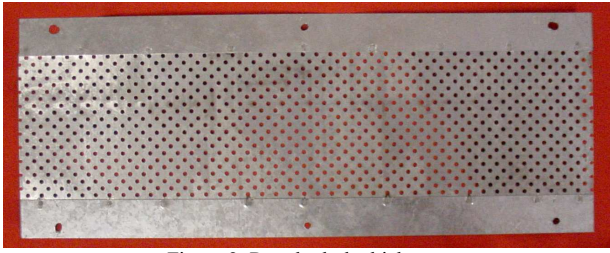


Figure 2. Regular hole thickener.

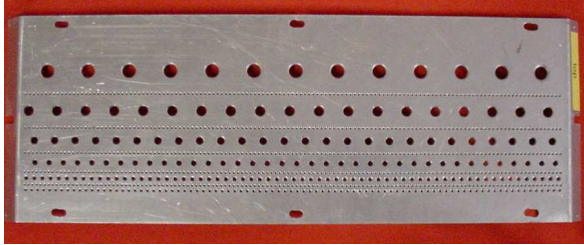


Figure 3. Varying hole thickener.

Hole dia (mm)	Total no. holes	No. Rows	Dist from leading edge (mm)	Lateral pitch (mm)
1.5	660	5	22.8, 43.3, 57.8, 68.0, 75.8	3.0
2.0	88	1	78.8	4.5
3.0	66	1	72.0	7.6
4.0	37	1	62.8	10.6
5.5	26	1	51.0	15.2
7.5	18	1	34.0	21.2
10.0	13	1	7.5	30.3

Table 1: Hole distribution for varying hole thickener (Fig 3.).

Experimental configuration

The closed circuit wind tunnel in the Aerodynamics Laboratory at the University of Tasmania was used for the present work. This wind tunnel has a 615mm square working section with corner fillets and length 1.2m. It is preceded by a 9:1 area ratio contraction of similar cross-section.

The boundary layer thickening plates were located upstream of the working section in as shown in the schematic in Figure 4. The wind tunnel was operated at nominally 23 m/s. The plates could be easily interchanged, and the air intake system removed when the fence thickener was used.

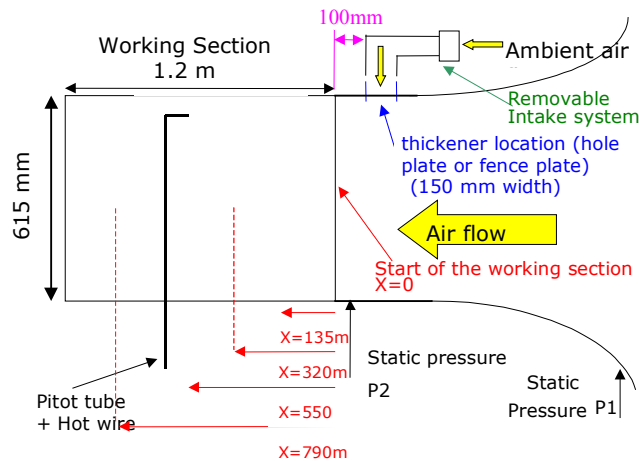


Figure 4. Wind tunnel configuration (not to scale).

The flow rate of ingested air was controlled by the pressure difference between ambient pressure and the lower static pressure

in the wind tunnel at the thickener location. The measured flow rates for the three different intake configurations are outlined in Table 2. The flow rates were nominally constant between hole configurations, at the maximum level possible with the pressure difference available. The influence of flow rate on boundary layer thickness will be the subject of future research.

	Q (m ³ /s)	q (m ³ /s/m)
Varying holes	0.0401	0.100
Regular holes	0.0420	0.104
Varying holes reversed	0.0408	0.101

Table 2. Secondary flow rate through hole thickeners.

A boundary layer traverse at the thickener location demonstrated that the undisturbed boundary layer was fully turbulent at the thickener location with a displacement thickness, $\delta^* = 1.03$ mm and boundary layer thickness Reynolds number, $Re_\theta = 1510$. The boundary layer was traversed with a 1.26mm diameter pitot tube and hot wire probes at distances 135, 320, 550 and 790 mm downstream from the start of the working section to study the development of the natural and perturbed boundary layers. The DISA 55M Constant Temperature Anemometer was used with a single axis hot wire probe (Dantec 55P11), with sensor normal to the mean flow.

Results

Boundary layer parameters

The boundary layer parameters for the natural boundary layer (no thickening) and the thickened boundary layers formed using the four thickening devices summarised in Table 3 demonstrate that all of the devices achieved some level of boundary layer thickening.

x	δ^* (mm)	θ (mm)	H	Re_θ	c_f
Natural					
135 mm	1.545	1.244	1.242	2900	0.00347
320 mm	2.067	1.630	1.268	3800	0.00326
550 mm	2.834	2.215	1.279	5160	0.00306
790 mm	3.848	3.033	1.269	7070	0.00292
Fence					
135 mm	4.891	3.698	1.323	8620	0.00266
320 mm	6.032	4.725	1.277	11010	0.00285
550 mm	6.391	5.124	1.247	11940	0.00292
790 mm	6.944	5.560	1.249	12960	0.00279
Varying holes					
135 mm	6.400	4.044	1.583	9420	0.00181
320 mm	6.419	4.554	1.410	10610	0.00230
550 mm	6.751	5.074	1.331	11820	0.00256
790 mm	7.172	5.525	1.298	12870	0.00260
Regular holes					
135 mm	5.430	3.719	1.460	8670	0.00213
320 mm	5.948	4.430	1.343	10320	0.00260
550 mm	6.793	5.308	1.280	12370	0.00285
790 mm	6.760	5.383	1.256	12540	0.00279
Varying holes reverse					
135 mm	5.511	4.040	1.364	9410	0.00254
320 mm	5.712	4.418	1.293	10290	0.00279
550 mm	6.178	4.900	1.261	11420	0.00285
790 mm	6.518	5.216	1.250	12150	0.00277

Table 3. Measured boundary layer parameters .

Momentum profiles

The velocity profiles at the end of the working section downstream of the boundary layer thickening devices are shown in Figure 5. At this location, the boundary layers are fully developed and there is little difference in the momentum thickness produced. The momentum deficit produced by the varying holes device is concentrated near the wall. The fence is more effective in producing a momentum deficit in the outer region of the boundary layer. The profiles downstream of the regular hole plate and the reversed varying hole plate are similar.

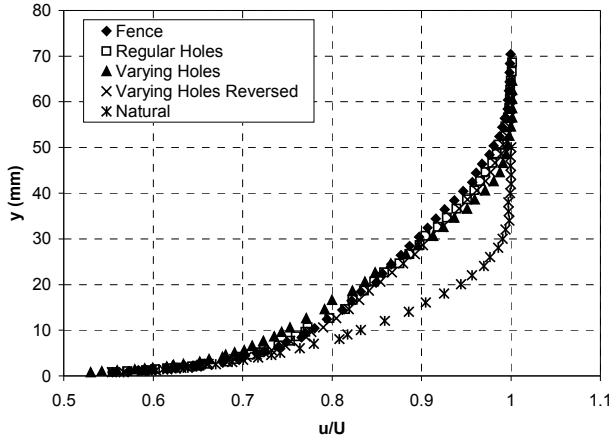


Figure 5. Velocity profiles for established boundary layers (790 mm).

The quality of the thickened boundary layer velocity distribution is determined by comparing with the standard law of the wall following Coles [4] with $K=0.393$ and $B=5.56$. The wall shear stress, τ_w , was measured using a 1.26mm diameter Preston tube (extending only into the transition region between the viscous sub-layer and fully turbulent log layer) with the calibration data provided by Patel [3]. An adjacent wall tapping provided the static pressure for the Preston tube measurement.

Hence the wall shear velocity, $u^* = (\tau_w / \rho)^{1/2}$, was determined and the velocity profiles could be compared using the inner-law variables:

$$u^+ = \frac{\ln y^+}{K} + B \quad \text{where } u^+ = \frac{u}{u^*} \quad \text{and } y^+ = \frac{yu^*}{\nu} \quad (1)$$

The thickened boundary layers all show a greater region of wall similarity (Figure 6) than the natural boundary layer, as might be expected from the higher Reynolds number for these cases. A small undershoot of the law of the wall is noticeable in the outer part of the wall layer for all the thickening devices. The wake region is very similar for the fence, regular holes and varying holes (reversed) devices. The varying holes thickener produced a significantly higher wake component with an associated increase in shape factor H .

Development of the momentum thickness and shape factor with distance downstream of the thickening devices is shown in Figures 7 and 8. The increase in momentum thickness is comparable for all the devices tested, but the variation with streamwise distance is less regular for the fence and varying holes devices.

The development of the boundary layer momentum thickness along the wind tunnel working section (Figure 7) highlights the dramatic increase in θ that can be achieved using these techniques. The increase in θ with downstream location for the regular holes does not appear to be monotonic, indicating that this technique may not be suitable for use with models requiring some development of the boundary layer.

The fence and the varying holes (reversed) show the most rapid return to an equilibrium condition, as demonstrated by the shape factor variation with streamwise distance (Figure 8). The boundary layer created by the varying holes plate demonstrated the largest disturbance of shape factor, which was not fully at equilibrium even at the downstream measurement location. The superior performance of the fence and varying holes reversed devices is clearly due to the fact that their initial perturbations from equilibrium are smaller in magnitude. The different performance of the injection devices, particularly the varying holes in normal and reversed configurations demonstrates that hole configuration is important in controlling the boundary layer.

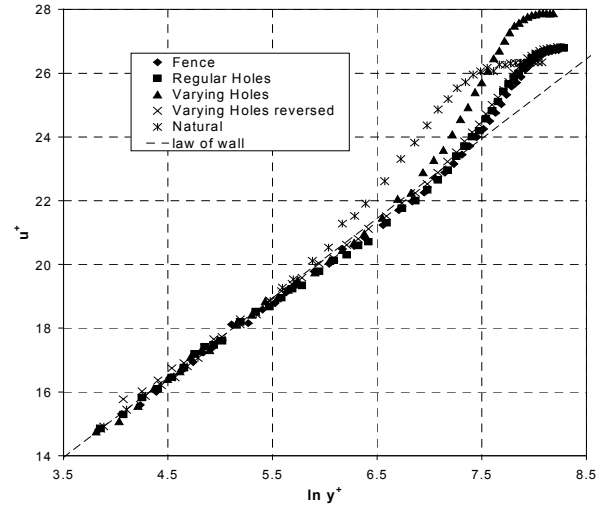


Figure 6. Velocity profiles compared with law of the wall (790 mm).

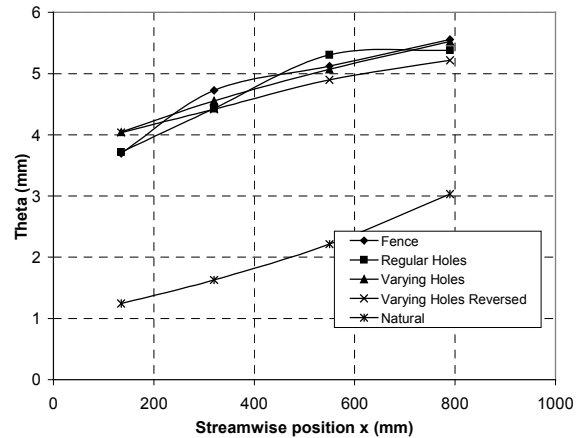


Figure 7. Development of boundary layer momentum thickness.

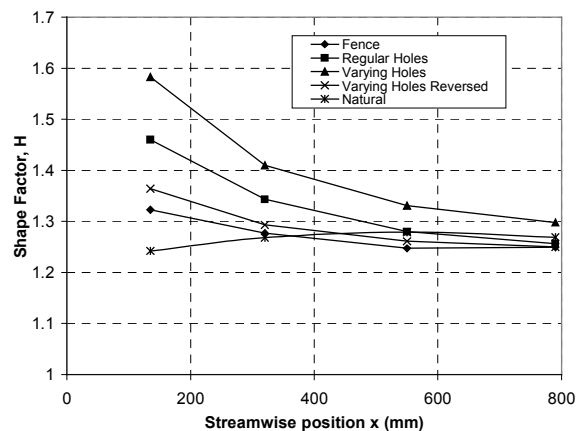


Figure 8. Development of boundary layer shape factor.

Turbulence Profiles

Figure 9 compares the turbulence profiles at $x = 550$ mm for the natural boundary layer and various thickening devices. The turbulence levels in the natural boundary layer slightly exceed those reported by Klebanoff [5] in the wall region. Wall vibration may have been a factor in this apparent increase.

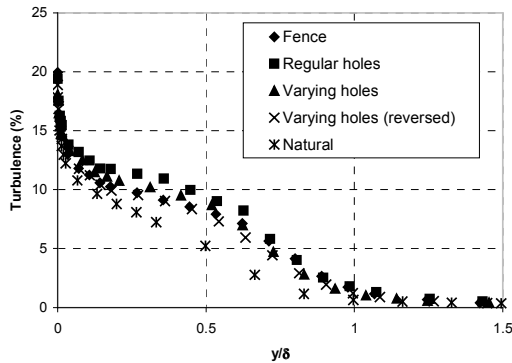


Figure 9. Comparison of turbulence profiles at $x=550$ mm for natural boundary layer and various thickening devices.

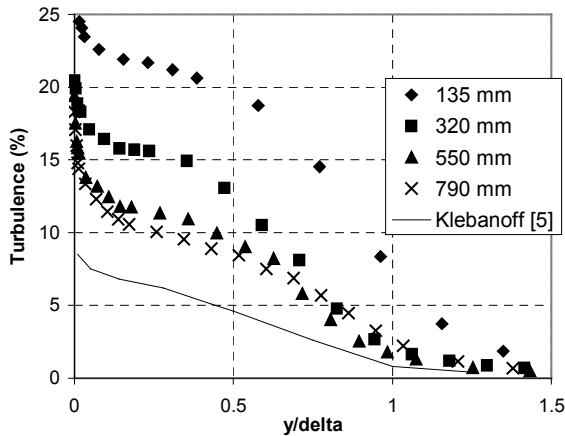


Figure 10. Turbulence profile for regular hole device boundary layers (Largest increase in b.l. turbulence).

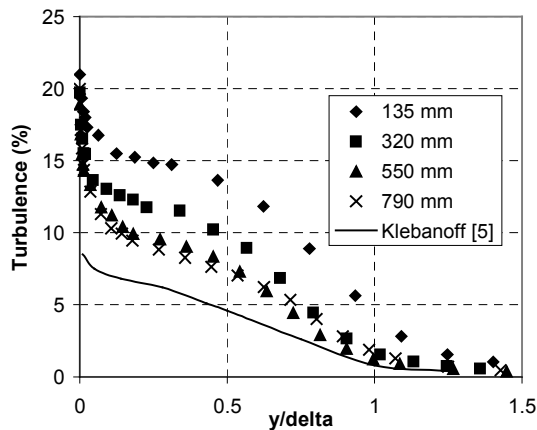


Figure 11: Turbulence profile for varying hole (reversed) device boundary layers (Smallest increase in b.l. turbulence).

All of the thickening methods produce an elevation of turbulence level over the natural boundary layer values for $0.2 < y/\delta < 0.7$. This increase in turbulence may be associated with the

streamwise vortex structure introduced to create the mixing required to produce the desired momentum profile.

Figures 10-11 show the streamwise development of boundary layer turbulence profiles for the regular holes and the varying holes (reversed) devices, which respectively produced the greatest and least turbulence elevation of all the thickening devices. The turbulence profiles have essentially stabilised by $x = 550$ mm, about 10δ (thickened) downstream of the device.

Conclusions

The present work has demonstrated that the boundary layer can be artificially thickened by naturally aspirating jets, or by a boundary layer fence. The momentum profiles have demonstrated that up to a trebling of the momentum and displacement thickness of the natural boundary layer can be achieved.

The passive serrated fence and active injection type devices were all found capable of producing comparable degrees of boundary layer thickening. The regular holes and varying holes device were less satisfactory in that they produced higher levels of turbulence and a slower return to equilibrium with distance downstream. The performance of the fence and varying holes (reversed) devices were closely comparable. These are capable of establishing a reasonably developed momentum boundary layer a distance of 10δ (thickened) downstream of the device. A trebling of the natural boundary layer thickness was achieved. All of the thickening devices produced significantly elevated turbulence levels in the central region of the boundary layer, which may be associated with the streamwise vortex structure introduced to achieve the required mixing.

The measured velocity and turbulence profiles in the artificially thickened boundary layers indicate that the preferred thickening devices are the fence and the array of jets with the largest jets downstream. This choice is based on obtaining a realistic velocity profile, compared with the law of the wall, and retaining a turbulence profile most similar to the natural boundary layer.

References

- [1] Roberts, J.L., The influence of hull boundary layers on waterjet intake performance, PhD thesis, University of Tasmania, 1998.
- [2] Roberts, J.L. and Walker, G.J., Artificial thickening of wind tunnel boundary layers via an array of cross-flow jets, *Experimental Thermal and Fluid Science*, **27**, 2003, 583-588.
- [3] Patel, V.C., Calibration of the Preston tube and limitations on its use in pressure gradients., *Journal of Fluid Mechanics*, **23**, 1965, 185-208.
- [4] Schlichting, H., 1979, "Boundary-Layer Theory", Seventh Edition, *McGraw-Hill Book Company*, New York.
- [5] Klebanoff, P.S., Characteristics of turbulence in a boundary layer with zero pressure gradient, NACA Rep. No. 1247, 1955.
- [6] Standen, N.M., A spire array for generating thick turbulent shear layers for natural wind simulation in wind tunnels, LTR-LA-94, National Aeronautical Establishment, NRC Canada, May 1972.